

ORIGINS OF COERCIVITY IN THE AMORPHOUS ALLOY Nd-Fe-Al

The relationship between nanostructure and coercivity in Nd-Fe-Al metallic glasses has been deduced from the x-ray diffraction data from the Advanced Photon Source and a variety of materials characterization techniques. The microstructural analyses show that the as-quenched alloys do not possess a homogeneously amorphous structure. Advanced transmission electron microscopy imaging techniques clearly show the existence of small clusters with a median size around 1.2 nm, while the x-ray diffraction data are consistent with at least two distinct short-range chemical orderings, resulting in two magnetic phases.

The ferromagnetic bulk metallic glass composition around $R_{60}Fe_{30}Al_{10}$ ($R = Nd$ or Pr) has generated considerable interest by virtue of its appreciable coercivity [1], an apparent contradiction to conventional understanding of the relationship between nanostructure and coercivity in amorphous materials. In technologically relevant materials, coercivity typically arises from impediments to domain wall motion, such as grain boundaries or other defects. The origin of impediments to domain wall motion is unclear in bulk amorphous magnetic alloys with high coercivities. Previous authors have speculated that the R-Fe-Al bulk metallic glasses possess short-range order that confers coercivity [2].

Recent work performed by the present authors, reported elsewhere [3], deduced the presence of highly stable nanoscopic aluminide and/or silicide phases, or motes, present in the melt prior to solidification of melt-spun, nominally amorphous alloys of $Nd_{60}Fe_{30}Al_{10}$. It was concluded that these motes would affect the short-range order and coercivity of the resultant glassy state, as well as provide heterogeneous nucleation sites for crystallization.

To pursue the characterization of clusters in the glassy matrix and to better understand the origin of coercivity in these materials, nominally homogeneous, amorphous samples of melt-spun $Nd_{60-2/3x}Fe_{30-1/3x}Al_{10+x}$ ($-2 < x < 2$) were studied

with a variety of diverse probes to characterize the material in its as-spun state as well as during *in situ* devitrification to clarify the relationship between the microstructure and the coercivity. The detailed structure of the glass was investigated using synchrotron x-ray diffraction (XRD) and advanced transmission electron microscopy (TEM) techniques. Ongoing parallel studies [4] have revealed a very close connection between the temperature-dependent magnetic behavior of a stable phase in the Nd-Fe-Al ternary phase diagram, $Nd_6Fe_{13-x}Al_{1+x}$ (also known as the δ phase) and the nominally amorphous melt-spun $Nd_{60}Fe_{30}Al_{10}$ ribbons.

The structure of the amorphous alloy as a function of temperature was studied using synchrotron radiation [5]. The *in situ* crystallization of the rapidly solidified ribbons was performed at the 6-ID-B beamline of the Advanced Photon Source located at Argonne National Laboratory in collaboration with the Midwest Universities Collaborative Access Team (MU-CAT). The data presented in this study were obtained with incident energies near 40 keV (0.3237 Å), selected using a double-crystal monochromator. The exact wavelength for each run was determined using a NIST Si standard (640b). The wavelength was determined using step scans over $\langle 111 \rangle$ to the $\langle 533 \rangle$ reflections above and below the horizontal. The image plates were calibrated by

exposing the entire plate to the Si standard and least squares fitting all the reflections for the entire plate to obtain the average distance from the sample. The melt-spun ribbons were ground into powder in an inert atmosphere and loaded into 2-mm-internal-diameter thin-walled amorphous silica tubes. Prior to sealing, the tubes were evacuated to a pressure $<10^{-2}$ mbar and then backfilled with argon. A Debye-Scherrer geometry (with an area detector) for collection of diffracted x-rays was employed. The detector was a 200×250 mm Fuji image plate with pixel dimensions of 100×100 μm . The image plates were translated across a 1-mm vertical slit aligned with the long dimension of the plate (see Sordelet et al. in this volume). Each spectrum was obtained by translating the plate 3 mm with the x-ray shutter open. The translation rate was 2.0 mm/s, for a total exposure time of 1.5 s. The sample was rotated $\pm 18^\circ$ during the exposure to improve powder averaging. Individual spectra were then obtained by averaging the 30-column-wide pixels. Intensity correction was determined using NBS intensity standard 674 Al_2O_3 taken in identical fashion. In this manner, up to 47 spectra could be obtained on each image plate. These studies show that there are unexpected subtle structural changes in the amorphous material that occur at temperatures well below the crystallization temperature of 780 K.

Data obtained from a variety of materials characterization techniques, in addition to synchrotron XRD, must be combined to yield a true picture of the Nd-Fe-Al microstructure. The microstructural analyses show that the as-quenched alloys do not possess a homogeneously amorphous structure. The TEM conical dark field (CDF) imaging techniques clearly show the existence of small clusters with a median size around 1.2 nm, while the XRD data are consistent with at least two distinct short-range chemical orderings, resulting in two magnetic phases. The synchrotron data facilitated identification of these two magnetic phases. Upon heating the as-quenched alloys, high-temperature transmission XRD shows formation of nanophased Nd in a persistent glassy matrix up to the crystallization temperature of 780 K (Fig. 1). The devitrified alloy contains primarily Nd and δ phases as expected from

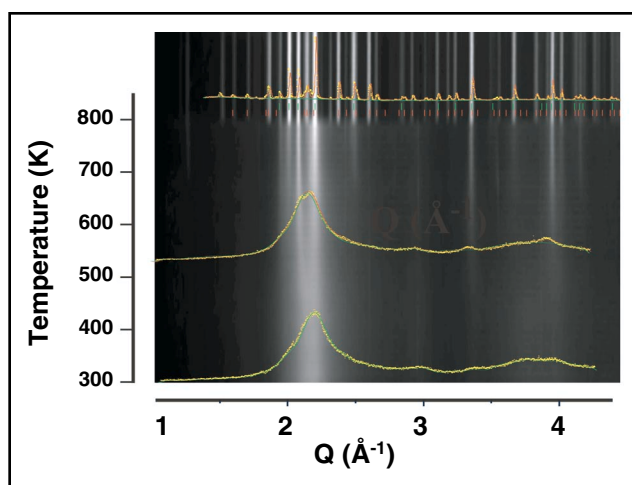


FIG. 1. Image plate showing the devitrification of $\text{Nd}_{60}\text{Fe}_{30}\text{Al}_{10}$ alloy heated from 300 K to 850 K at 10 K/min with a short hold time at 850 K. Overlaid on the image plate are representative Rietveld scans at 300, 530, and 850 K. The as-quenched alloy is modeled with only diffuse scattering. The 530 K scan shows formation of coherent scattering clusters of Nd. At 780 K, coherent scattering from the δ phase is observed. The reflections from the Nd phase are indicated by green hash marks, while the reflections of the δ phase are indicated by red hash marks.

the equilibrium phase diagram. Rietveld refinement of XRD data extracted from the image plate at temperatures of 300 K, 530 K, and 850 K are shown as insets on the image plate (Fig. 1). Near 500 K, but still below the bulk crystallization temperature of the material, clusters of Nd begin to form and to coherently scatter the incident synchrotron radiation. The size of the Nd clusters increases with heating. Thus one of the two distinct magnetic phases is Nd. The composition of the other cluster type is deduced from the magnetic properties of the as-quenched ribbon. The significant magnetic hysteresis observed in the magnetically hard fraction of the sample requires a large uniaxial anisotropy; however, the temperature dependence of the coercivity differs from that of a homogeneous material with random uniaxial anisotropy. In a homogeneous material, coercivity tends to decrease at a faster rate than does the magnetization with increasing temperature but does not disappear until the ferromagnetic transition temperature, or Curie temperature (T_c). This type of magnetic behavior is not observed in these alloys. In fact, the onset of coercivity near $0.5 T_c$ is better

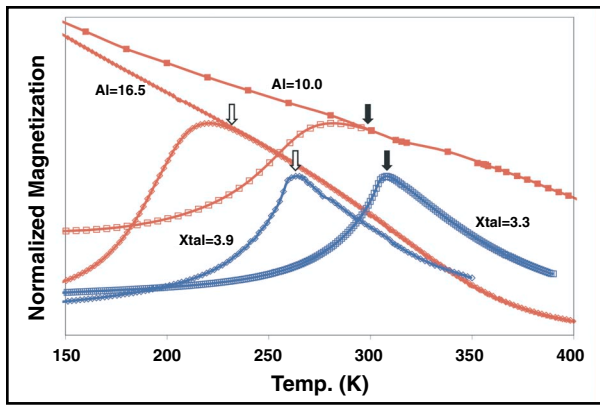


FIG. 2. Field-cooled (FC) and zero-field-cooled (ZFC) magnetization measurements of the as-quenched alloys of varying Al content (shown in red) and FC measurements of single crystals ($H \parallel c$) at the expected composition for primary solidification of the δ phase (shown in blue). Note the correlation between the onset of hysteresis and the Néel temperature (arrows) of the single crystals to that of as-quenched alloys and their similar compositional dependence (closed and open arrows).

explained by “exchange bias”-type magnetic coupling, in which a soft ferromagnetic phase is exchange-coupled to an antiferromagnetic phase. In the case where the antiferromagnetic transition temperature, or Néel temperature (T_N), is lower than T_c , the soft phase will have shown no coercivity in the temperature region $T_N < T < T_c$ but will develop coercivity rapidly when the temperature falls below T_N . Thus the onset of coercivity for ribbons of different compositions should scale with the Néel temperature T_N of the primary δ composition (Fig. 2).

This result is indeed observed, and it is therefore probable that the other magnetic phase is closely related to the δ phase.

While the clusters observed in the TEM CDF images are large compared to those observed in other metallic glasses, they are clearly smaller than the unit cell of the primary solidification δ phase, which has a complex tetragonal structure with $a = 0.80$ nm and $c = 2.28$ nm [6]. The complex relationships between magnetic anisotropy, chemical bonding, and cluster size in crystalline alloys of composition $\text{Nd}_6\text{Fe}_{13-x}\text{Al}_{1+x}$ are topics of future investigation.

Principal publication: “Origins of Coercivity in the Amorphous Alloy Nd-Fe-Al,” *J. Appl. Phys.*, in press.

REFERENCES

- [1] A. Inoue, T. Zhang, W. Zhang, and A. Takeuchi, *Materials Trans.*, **JIM** **37**, 99 (1996).
- [2] A. Inoue, A. Takeuchi, and T. Zhang, *Met. Mater. Trans. A* **29A**, 1779-1793 (1998).
- [3] A.S. O'Connor, L.H. Lewis, R.W. McCallum, K.W. Dennis, M.J. Kramer, D.T. Kim Anh, N.H. Dan, N.H. Luong, and N.X. Phuc, *JIM Proc.* **14** Proc. of the 16th International Workshop on Rare-Earth Magnets and Their Applications, vol. 1 (2000) pp. 475-482.
- [4] R.W. McCallum, I.R. Fisher, N.E. Anderson, P.C. Canfield, M.J. Kramer, and K.W. Dennis, *IEEE Trans. Mag.*, **37**, 4 2147-2149 (2001).
- [5] L. Margulies, M.J. Kramer, R.W. McCallum, S. Kycia, D.R. Haeffner, J.C. Lang, and H.I. Goldman, *Rev. Sci. Instrum.* **70**, 3554 (1999).
- [6] J. Allemand, A. Letant, J.M. Moreau, J.P. Nozieres, and P. de la Bathie, *J. Less Comm. Met.* **166**, 73 (1990).

M. J. Kramer,¹ A. S. O'Connor,¹ K. W. Dennis,¹ R. W. McCallum,¹ L. H. Lewis,² L. D. Tung,³ N. P. Duong³

¹ Ames Laboratory, U.S. DOE and Department of Materials Science and Engineering, Iowa State University, Ames, IA, U.S.A.

² Materials and Chemical Sciences Division, Energy Sciences and Technology Department, Brookhaven National Laboratory, Upton, NY, U.S.A.

³ International Training Institute for Materials Science, Hanoi, Vietnam